NASA/TM—2020-220384

Control Demonstration of Multiple Doubly Fed Induction Motors for Hybrid Electric Propulsion

David J. Sadey
Glenn Research Center, Cleveland, Ohio

Marc Bodson
University of Utah, Salt Lake City, Utah

Jeffrey T. Csank, Keith R. Hunker, Casey J. Theman, and Linda M. Taylor
Glenn Research Center, Cleveland, Ohio

December 2020

NASA STI Program . . . in Profile

Since its founding, NASA has been dedicated to the advancement of aeronautics and space science. The NASA Scientific and Technical Information (STI) Program plays a key part in helping NASA maintain this important role.

The NASA STI Program operates under the auspices of the Agency Chief Information Officer. It collects, organizes, provides for archiving, and disseminates NASA's STI. The NASA STI Program provides access to the NASA Technical Report Server—Registered (NTRS Reg) and NASA Technical Report Server—Public (NTRS) thus providing one of the largest collections of aeronautical and space science STI in the world. Results are published in both non-NASA channels and by NASA in the NASA STI Report Series, which includes the following report types:

- TECHNICAL PUBLICATION. Reports of completed research or a major significant phase of research that present the results of NASA programs and include extensive data or theoretical analysis. Includes compilations of significant scientific and technical data and information deemed to be of continuing reference value. NASA counter-part of peer-reviewed formal professional papers, but has less stringent limitations on manuscript length and extent of graphic presentations.

- TECHNICAL MEMORANDUM. Scientific and technical findings that are preliminary or of specialized interest, e.g., "quick-release" reports, working papers, and bibliographies that contain minimal annotation. Does not contain extensive analysis.

- CONTRACTOR REPORT. Scientific and technical findings by NASA-sponsored contractors and grantees.

- CONFERENCE PUBLICATION. Collected papers from scientific and technical conferences, symposia, seminars, or other meetings sponsored or co-sponsored by NASA.

- SPECIAL PUBLICATION. Scientific, technical, or historical information from NASA programs, projects, and missions, often concerned with subjects having substantial public interest.

- TECHNICAL TRANSLATION. English-language translations of foreign scientific and technical material pertinent to NASA's mission.

For more information about the NASA STI program, see the following:

- Access the NASA STI program home page at http://www.sti.nasa.gov

- E-mail your question to help@sti.nasa.gov

- Fax your question to the NASA STI Information Desk at 757-864-6500

- Telephone the NASA STI Information Desk at 757-864-9658

- Write to:
  NASA STI Program
  Mail Stop 148
  NASA Langley Research Center
  Hampton, VA 23681-2199

NASA/TM—2020-220384

Control Demonstration of Multiple Doubly Fed Induction Motors for Hybrid Electric Propulsion

David J. Sadey
Glenn Research Center, Cleveland, Ohio

Marc Bodson
University of Utah, Salt Lake City, Utah

Jeffrey T. Csank, Keith R. Hunker, Casey J. Theman, and Linda M. Taylor
Glenn Research Center, Cleveland, Ohio

National Aeronautics and
Space Administration

Glenn Research Center
Cleveland, Ohio 44135

December 2020

Acknowledgments

The authors would like to thank the NASA Convergent Aeronautics Solutions (CAS) project and Ray Beach in support of this effort, along with Jim Dolce, Tom Balogas, David Hausser, and George Horning for their assistance in the construction of the low-power testbed.

This work was sponsored by the
Transformative Aeronautics Concepts Program.

Level of Review: This material has been technically reviewed by technical management.

Available from

NASA STI Program
Mail Stop 148
NASA Langley Research Center
Hampton, VA 23681-2199

National Technical Information Service
5285 Port Royal Road
Springfield, VA 22161
703-605-6000

This report is available in electronic form at http://www.sti.nasa.gov/ and http://ntrs.nasa.gov/

Control Demonstration of Multiple Doubly Fed Induction Motors for Hybrid Electric Propulsion

David J. Sadey
National Aeronautics and Space Administration
Glenn Research Center
Cleveland, Ohio 44135

Marc Bodson
University of Utah
Salt Lake City, Utah 84112

Jeffrey T. Csank, Keith R. Hunker, Casey J. Theman, and Linda M. Taylor
National Aeronautics and Space Administration
Glenn Research Center
Cleveland, Ohio 44135

Summary

The Convergent Aeronautics Solutions (CAS) High Voltage Hybrid Electric Propulsion (HVHEP) activity was formulated to support the move into future hybrid-electric aircraft. The goal of this high-voltage activity is to develop a new alternating current (AC) power architecture to support the needs of higher efficiency and lower emissions aircraft. This proposed architecture will adopt the use of the doubly fed induction machine (DFIM) for propulsor drive motor application. The DFIMs are attractive for several reasons, including but not limited to, the ability to self-start, the ability to operate subsynchronously and supersynchronously, and the requirement for power converters rated at a fraction of those required in a corresponding direct current system, dependent on the range of operation. The focus of this report is based specifically on the presentation and analysis of a novel strategy, which allows for independent operation of multiple doubly fed induction motors from a common AC bus. This strategy includes synchronization, soft-start, and closed-loop speed control of each motor as a means of controlling output thrust, be it concurrently or differentially. The demonstration of this strategy has recently been proven on a low-power testbed using fractional horsepower machines. Simulation and hardware test results are presented in this report.

Nomenclature

3ϕ	three phase
AC	alternating current
ARMD	Aeronautics Research Mission Directorate
CAS	Convergent Aeronautics Solutions
Cmd	command
COTS	commercial off the shelf
DC	direct current
DFI	doubly fed induction
DFIM	doubly fed induction machine
Gen.	generator

HVHEP	High Voltage Hybrid Electric Propulsion
I_S^*	stator current phasor, A peak
I_R^*	rotor current phasor, A peak
M1…M3	motor 1 to motor 3
N.O.	normally open
n_P	number of pole pairs
n_S	synchronous speed, rpm
$\overline{P}_{CONV}$	regenerated RSC power
P_M	mechanical rotor power, W
$\overline{P}_M$	per-unit mechanical rotor power
PMDC	Permanent magnet direct current
P_R	electrical rotor power, W
$\overline{P}_R$	per-unit rotor power
P_S	stator power, W
$\overline{P}_S$	per-unit stator power
pf	unity stator power factor
Q_R	rotor reactive power, VAR
Q_{REF}	second outer loop power reference
Q_S	stator reactive power, VAR
RSC	rotor-side converter
RMS	root mean square
s	per-unit slip
sync.	synchronous
t	time
v_G	grid voltage vector
VLL	line-to-line voltage
V_R	rotor voltage phasor, V peak
v_R	rotor voltage vector
V_S	stator voltage phasor, V peak
v_S	stator voltage vector
θ_M	rotor angle, rad
τ	torque
τ_{COM}	torque command
ω_M	rotor speed, rad/s
$\overline{\omega}_R$	per unit rotor speed, rad/s
ω_{REF}	speed control tacking reference
ω_S	synchronous electrical angular frequency, rad/s

1.0 Introduction

The NASA Aeronautics Research Mission Directorate (ARMD), and the aeronautics industry as a whole, is constantly being challenged to achieve reductions in noise, emissions, and fuel burn over today's current aircraft (Ref. 1). One of the possible paths forward focuses on partial to complete electrification of the aircraft, depending on size and mission duration. The current approach within the ARMD towards further electrification of aircraft has focused on a primarily direct-current- (DC-) based

transmission system (Ref. 2), as shown in Figure 1. This system relies on multiple power conversion stages to transmit the alternating current (AC) power extracted from the turbine driven generator(s) to the AC motor(s) driving the propulsor fan(s). The power must be converted from AC to DC and then back to AC, which requires two stages of full power rated converters; these converters have a large negative impact on the total system weight and efficiency. To overcome this negative impact, the NASA Convergent Aeronautics Solutions (CAS) High Voltage Hybrid Electric Propulsion (HVHEP) activity has proposed a primarily AC system, which adopts the use of doubly fed induction machines (DFIMs), as shown in Figure 2. This DFIM-based AC system allows for the fully rated power converters of the DC system to be replaced with converters a fraction of the size. These AC converters are only required on the rotors of the DFIMs, resulting in overall weight savings and efficiency improvements. At the same time, the use of DFIMs, as opposed to synchronous machines, enables operation with an electrical frequency that is largely decoupled from the speed of the generator(s) and motor(s). This report will present a short overview of this system (Section 2.0), describe its operational characteristics and advantages (Section 3.0), and then present simulation (Section 4.0) and hardware results (Section 5.0) based on the independent operation of the downstream propulsor motors.

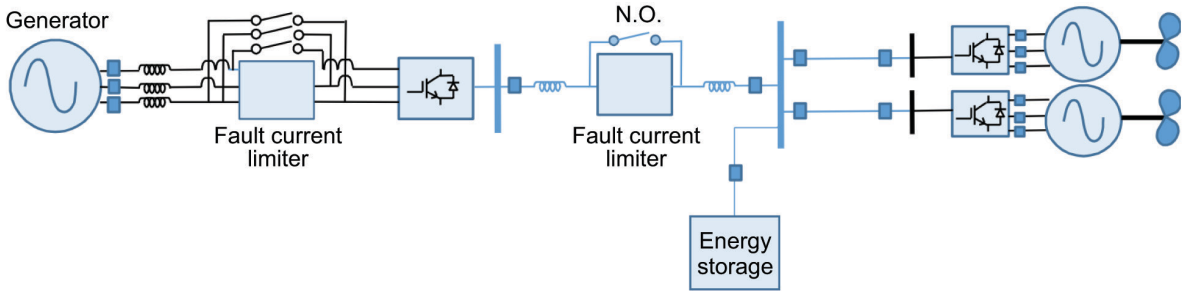

Figure 1.—Simplified baseline direct current power architecture (Ref. 2). Normally open (N.O.).

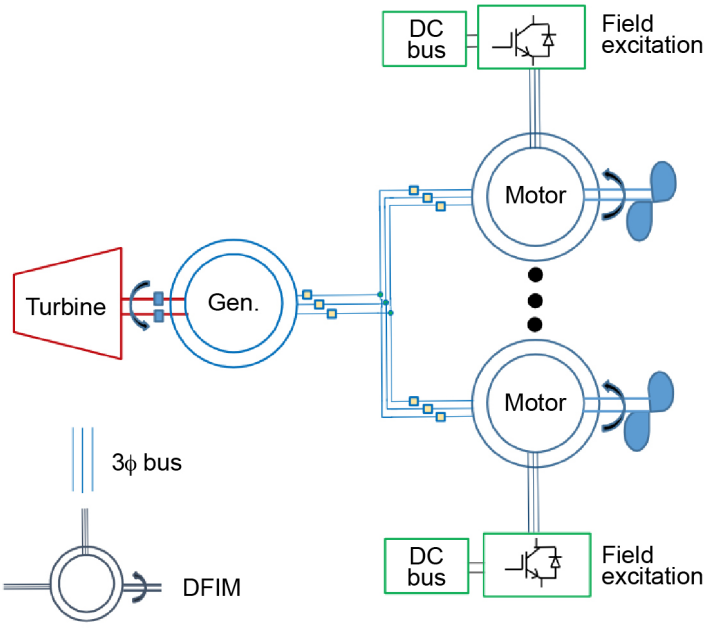

Figure 2.—Doubly fed induction machine- (DFIM-) based alternating current power architecture. Direct current (DC). Generator (Gen.). Three phase (3ϕ).

2.0 System Description

In the proposed AC system, which was originally described in Reference 3 and as seen in Figure 2, a gas turbine engine acts as a prime mover to an AC generator[1]. The generator then converts that mechanical power to three-phase electric power on its stator. Through the unique nature of the doubly fed induction (DFI) motor, the stator of the generator is directly connected to the stator of the individual motors via a three-phase transmission and distribution bus. The DFI motors, which will be described in detail in Section 3.0, are then independently controlled through the use of a rotor-side converter (RSC) to drive the propulsors of the aircraft. This system allows for individual control of the fans such that they can operate either in concurrence with one another, or differentially.

3.0 Doubly Fed Induction Motors

The DFIM is a unique machine, which has historically been used in wind turbine (Ref. 4) applications as a generator but has use as a motor as well. This machine has both stator and rotor windings where power can be actively injected or extracted. As previously stated, one advantage of the DFI motor is that it can be designed and exploited in such a way that the power electronics necessary to control the motor are relegated to the low-power rotor windings, thus reducing the required size of the power converter itself. In the configuration studied, the stator is directly coupled to a three-phase electric power source (electric grid), while the rotor uses a low-power, partially rated power converter to achieve variable speed operation of the machine. This section will describe the electric and mechanical theory relative to the machine, how the voltage and power of the RSC vary as a function of slip, and how the machine is controlled.

3.1 Doubly Fed Induction Motor Theory

Figure 3 shows the structure of a DFI motor. There is a side view of the motor (a) and a cross section of the motor (b), showing three-phase stator windings and three-phase rotor windings (in a simplified representation). The voltages applied to the stator windings are labeled $v_{a,S}$, $v_{b,S}$, and $v_{c,S}$, while the voltages applied to the rotor are labeled $v_{a,R}$, $v_{b,R}$, and $v_{c,R}$. The rotor voltages are applied through slip rings, as shown in Figure 3(a). The angle of the rotor winding a,R with respect to the stator winding a,S defines the rotor angular position, denoted θ_M, while the angular velocity is denoted $\omega_M = d\theta_M/dt$.

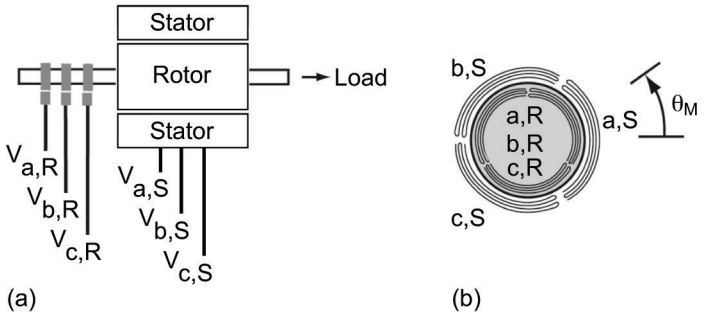

Figure 3.—Doubly fed induction (DFI) motor structure. (a) side view. Stator windings are labeled $v_{a,S}$, $v_{b,S}$, and $v_{c,S}$, while the voltages applied to the rotor are labeled $v_{a,R}$, $v_{b,R}$, and $v_{c,R}$. (b) Cross section. Rotor angular position (θ_M). Rotor (R). Stator (S).

[1]It is important to note that the generator may or may not be a DFIM as described in Reference 3, and the choice of generator type will depend on the power system architecture and system requirements. Implementing the DFIM as a generator as well may offer additional benefits, but is beyond the scope of this report.

In steady state, the stator voltages are sinusoidal variables with frequency ω_S, and can be represented by a single complex variable V_S (typically called a phasor) such that

$$v_{a,S} = \mathrm{Re}\left(V_S e^{j\omega_s t}\right) \tag{1}$$

$$v_{b,S} = \mathrm{Re}\left(V_S e^{j\omega_s t - j2\pi/3}\right) \tag{2}$$

$$v_{c,S} = \mathrm{Re}\left(V_S e^{j\omega_s t + j2\pi/3}\right) \tag{3}$$

The total active (P_S) and reactive (Q_S) power absorbed by the stator windings can be expressed as

$$P_S + jQ_S = \frac{3}{2} V_S I_S^* \tag{4}$$

where I_S^* is the complex conjugate of the phasor for the stator current. Similarly, the rotor voltages are sinusoidal variables with frequency $s\omega_S$, where s is the per-unit slip defined as

$$s = 1 - \frac{n_p \omega_M}{\omega_S} \tag{5}$$

and n_P is the number of pole pairs of the motor (n_P is equal to 1 in Figure 1). Note that the rotor electrical frequency, $s\omega_S$, can be negative, which corresponds to a phasor voltage rotating in the counterclockwise direction, that is, three-phase rotor voltages in reverse or backward sequence. Defining rotor voltage (V_R) and current (I_R^*) phasors, the total active (P_R) and reactive (Q_R) powers absorbed by the rotor are equal to

$$P_R + jQ_R = \frac{3}{2} V_R I_R^* \tag{6}$$

Neglecting losses in the motor, the mechanical power of the motor (P_M) is a function of the electrical power supplied to the stator and rotor windings:

$$P_M = \tau \omega_M = P_S + P_R \tag{7}$$

where τ is the torque and $\tau\omega_M$ is the mechanical power produced by the motor. It is also possible for electrical power to be absorbed by the stator windings and produced by the rotor windings (when $P_R < 0$). An interesting property of the DFI motor is that it can operate in subsynchronous or supersynchronous modes relative to the grid frequency. This means that while a conventional synchronous machine may operate at only one speed per given stator frequency (called synchronous speed), the DFI motor has the ability to operate below, at, or above this synchronous speed. In addition, the distribution of power is solely determined by the relative speed of the motor compared to the frequency of the stator input. Specifically, still neglecting losses, it turns out that

$$P_S = \frac{\omega_S}{n_P \omega_M} P_M \tag{8}$$

$$P_R = \frac{n_P \omega_M - \omega_S}{\omega_S} P_S = \frac{n_P \omega_M - \omega_S}{n_P \omega_M} P_M \tag{9}$$

Therefore, for positive torque and speed, $P_S > 0$ and $P_R > 0$ for $n_P\omega_M > \omega_S$ (the supersynchronous case with $s < 0$) while $P_S > 0$ and $P_R < 0$ for $n_P\omega_M < \omega_S$ (the subsynchronous case with $s > 0$).

3.2 Doubly Fed Induction Motor Converter Characteristics for Fan Loads

The converter for the DFI motor, which is sometimes referred to as the "RSC," is typically sized with regard to the operating characteristics of the machine along with the torque-speed (and therefore power) characteristics of the load. While there are numerous ratings and design criteria for the RSC to operate properly according to the system specification, this section focuses specifically on how the voltage and power characteristics of the RSC are derived for fan loads.

The voltage requirement of the RSC is directly proportional to the speed range of the rotor. At standstill, the induced voltage at the terminals of the rotor is at maximum. As the rotor speed increases, the rotor voltage linearly decreases from its maximum value to zero at synchronous speed (Ref. 5). With further increasing speed, the rotor voltage linearly increases back to its open circuit voltage at 200 percent rated speed. This voltage-speed characteristic is shown in Figure 4.

The voltage-speed characteristic of the DFI motor may be advantageous in applications where aircraft propulsors require only a limited speed range to operate. For example, if the required speed range is 15 percent about synchronous speed, the voltage requirement of the RSC would only be 0.15 per unit of the open circuit rotor voltage. This would in turn force a requirement for the stator bus to be a variable frequency bus, or to have a mechanical or electrical starting mechanism for the machine (e.g., crowbar circuit), but those requirements are beyond the scope of this report.

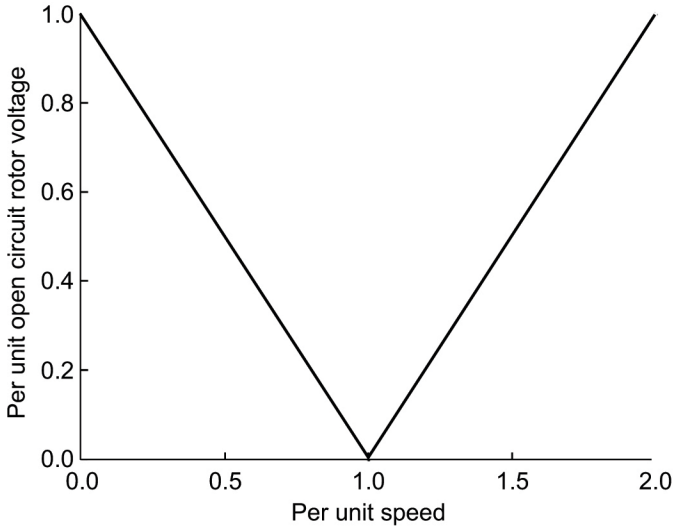

Figure 4.—Rotor voltage-speed characteristic curve.

As mentioned previously, the power characteristic of the RSC is related to the torque-speed characteristics of the fan load, along with the characteristics of the DFI motor itself. References 5 and 6 show the torque required to drive a fan load is actually proportional to the speed squared, which results in Equations (10) to (12) describing the DFI motor, stator, and rotor powers on a per-unit basis, respectively. The regenerated RSC power, $\overline{P}_{CONV}$, in per unit of the rated machine power, is given by Equation (12) as well.

$$\overline{P}_M = \overline{\omega}_R^3 \tag{10}$$

$$\overline{P}_S = \overline{\omega}_R^2 \tag{11}$$

$$\overline{P}_R = -\overline{P}_{CONV} = \overline{\omega}_R^3 - \overline{\omega}_R^2 \tag{12}$$

The relationship between the stator, rotor, and mechanical power as described by Equations (10) to (12) was shown by Reference 5 for subsynchronous operation. The Figure 5 plot is extended to supersynchronous operation (15 percent over synchronous speed). The red line shows the mechanical power ($\overline{P}_M$), the dotted black line shows the regenerated rotor power ($\overline{P}_{CONV}$), and the blue line shows the stator electrical power ($\overline{P}_S$). It is important to recognize that if zero to full speed operation were required for the machine, along with self-starting, the steady-state power processed by the RSC would only need to be approximately 15 percent of the rated power of the machine. In other words, because the power absorbed by a fan load is proportional to the cube of the speed, the range of speed for which a 15 percent RSC is applicable covers the whole subsynchronous speed range. Conversely, for supersynchronous speeds, the range is shortened, but the machine can still operate up to 12 percent above rated speed. These operating points are identified as the square and circle, respectively, in Figure 5.

As a summary, the voltage requirement of the RSC is defined by the speed range and open circuit voltage of the rotor (with the stator fully excited). The total power processed is defined by Equation (12). Ignoring accelerating power, this results in a reduction of at least 85 percent in power converted by the converters as compared to the DC baseline architecture, with an increased speed range of 12 percent without the requirement for field weakening over the baseline as well. Additional speed capability is possible, but depends on the operational characteristics and requirements of the system.

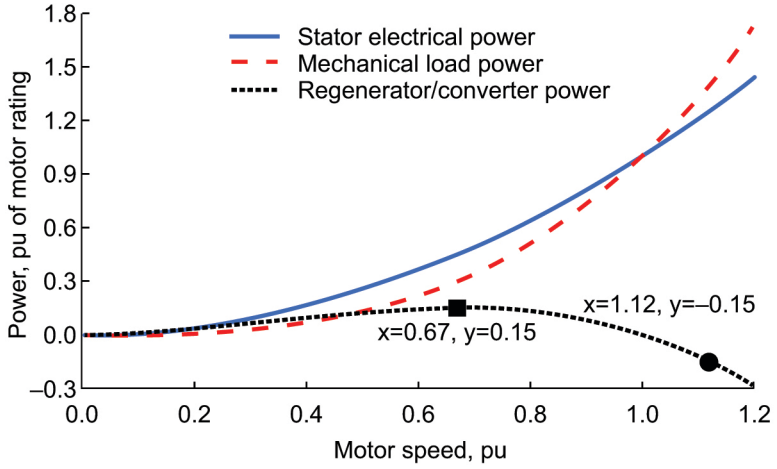

Figure 5.—Power curves doubly fed induction motor.

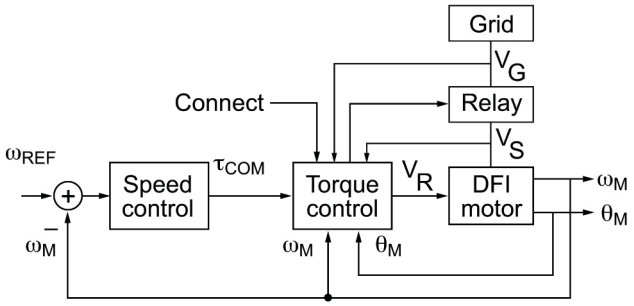

Figure 6.—Speed control algorithm. Doubly fed induction (DFI). Reference command (ω_{REF}). Rotor velocity (ω_M). Stator voltage vector (v_S). Grid voltage vector (v_G). Rotor voltage vector (v_R). Rotor position (θ_M). Torque command (τ_{COM}).

3.3 Doubly Fed Induction Motor Control

Figure 6 shows a block diagram of a control algorithm for the DFI motor. The stator windings are connected to a three-phase grid through a relay. In a turboelectric application, the grid is provided by a generator, possibly of a doubly fed induction type. The torque control block serves both to synchronize the machine to the grid before connection and to control the torque of the motor when connected. The vector of rotor voltages $v_R = (v_{a,R}\ v_{b,R}\ v_{c,R})^T$ is computed to provide a torque equal to the command τ_{COM} while absorbing zero stator reactive power ($Q_S = 0$). The computation is based on measurements of the rotor position θ_M, of the rotor velocity ω_M, and of the stator voltage vector $v_S = (v_{a,S}\ v_{b,S}\ v_{c,S})^T$. Before connection to the grid, the grid voltage vector $v_G = (v_{a,G}\ v_{b,G}\ v_{c,G})^T$ is also measured, and the rotor voltage vector is computed to ensure that $v_S = v_G$. This situation corresponds to a zero torque and zero reactive power, implying zero stator currents and, therefore, a possible connection to the grid with zero transients. When the voltages are equal, the operator triggers the "connect" variable, which closes the relay between the grid and the DFI motor. The connection can also be performed automatically.

The inner torque control algorithm is augmented by an outer loop for speed control that ensures the tracking of a reference command ω_{REF} by the speed ω_M. The speed control algorithm is a conventional proportional-integral control system with antiwindup protection. The torque command is limited to ensure that the predicted rotor currents stay within their limits.

In Figure 6, the rotor voltages are computed to produce a given torque with zero absorbed stator reactive power (all reactive power required by the magnetizing current is provided by the RSC to the rotor). However, an extension of the algorithm could enable the control of the reactive power using a second outer loop with reference Q_{REF} and a feedback of the stator reactive power based on measurements of the stator and rotor currents (not shown in Figure 6).

4.0 Simulation Results

To demonstrate and evaluate the general performance of the aforementioned control structure, a simple single-string model of the DFI motor was developed, as shown in Figure 7. The DFI motor is coupled to a permanent magnet DC (PMDC) machine that acts as a load. The characteristics of these machines are listed in Table 1 and Table 2 and were taken from nameplate and test data of commercial off-the-shelf (COTS) hardware procured for testing and simulation.

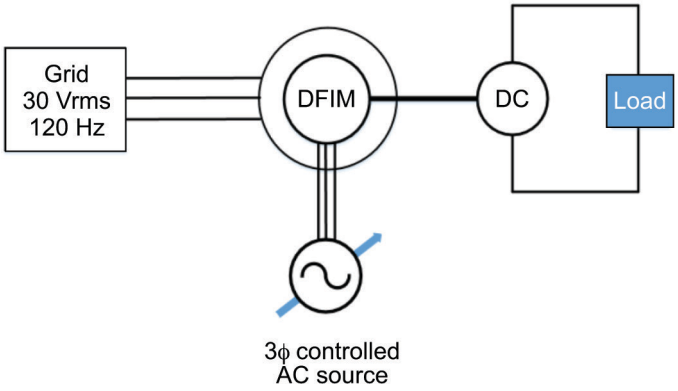

Figure 7.—Single-string doubly fed induction (DFI) motor test setup. Alternating current (AC). Direct current (DC). Doubly fed induction machine (DFIM). Three phase (3ϕ).

TABLE 1.—DOUBLY FED INDUCTION MOTOR CHARACTERISTICS

Parameter	
Rated power, W	250
Rated stator voltage, V	30
Rated frequency, Hz	120
Synchronous speed, rpm	3,600
Pole pairs	2
Stator inductance, mH[a]	2.5
Stator resistance, Ω[a]	0.6
Mutual inductance, mH[a]	6.6
Rotor inductance, mH[a]	0.24
Rotor resistance, Ω[a]	1.21
Stator connection	Star
Rotor connection	Delta

[a]All electrical parameters are referred to as the "stator side."

TABLE 2.—DIRECT CURRENT MACHINE CHARACTERISTICS

Parameter	
Rated power, W	250
Rated voltage, V	42
Rated speed, rpm	4,000
Pole pairs	1
Armature resistance, Ω	0.52
Armature inductance, mH	2.7

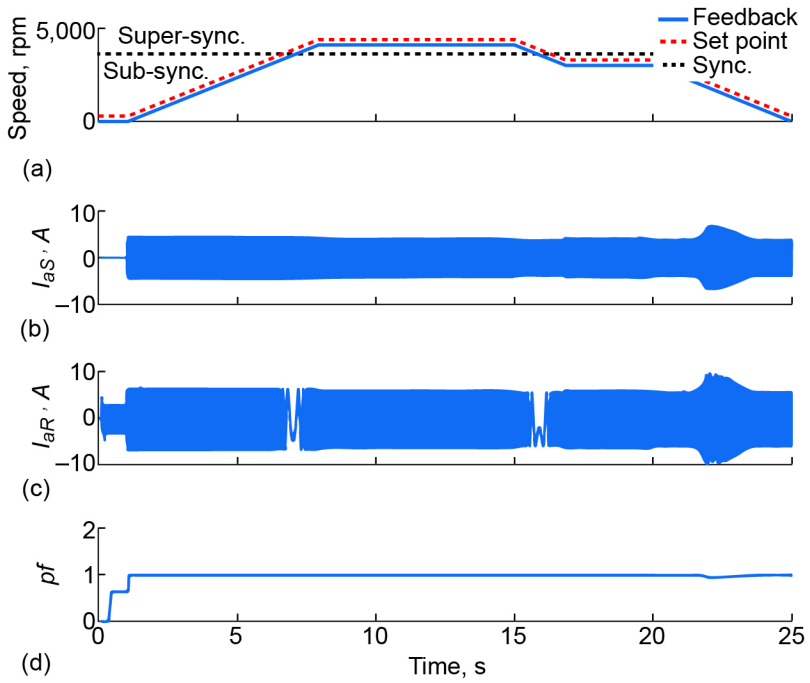

Figure 8.—Simulation results for single-string doubly fed induction motor test. (a) Speed reference tracking. Synchronous (sync). (b) Stator current (I_{aS}). (c) Rotor current (I_{aR}). (d) Unity stator-power factor control (*pf*).

Loading in the simulation was performed with a constant maximum torque load, as the ability to implement a dynamic fan load torque-speed characteristic was not possible with the hardware used in Section 5.0. The control algorithm was tuned for both the speed and reactive power control loops, in which acceptable performance was observed. The results of the simulation are shown in Figure 8, in which the machine is shown to have synchronized, self-started, transitioned through subsynchronous, synchronous, and supersynchronous modes, and automatically controlled its reactive power to obtain unity power factor operation at the stator.

5.0 Hardware Results

To evaluate the proposed system and its control, a low-power testbed was constructed using COTS hardware. The testbed power hardware included three fractional horsepower DFI motors, three inverters (42-V and three-phase), three PMDC machines to act as dynamometers, and a three-phase power supply. Figure 9 and Figure 10 show the testbed configuration and the power hardware, respectively. The testbed motors are configured in such a way as to represent a distributed propulsor-based aircraft. The system configuration was selected to demonstrate the ability for the motors to operate in parallel, both for concurrent and differential operation, and for convenience and cost purposes. It is important to note that during the hardware testing, it was observed that the DFI motors could not output as much power (only approx. 100 W) as was specified on the nameplate. Furthermore, bandwidth restrictions in hardware limited the ability to follow a desired fan-type torque-speed curve dynamically. These restrictions, in addition to slightly differing characteristics across machines, led to the application of a linear torque-speed curve (resistor on the dynamometer) versus the previously discussed fan load. Despite these limitations, the ability of the machines to synchronize to the main bus, self-start, operate concurrently and differentially, and follow a theoretical flight profile was demonstrated.

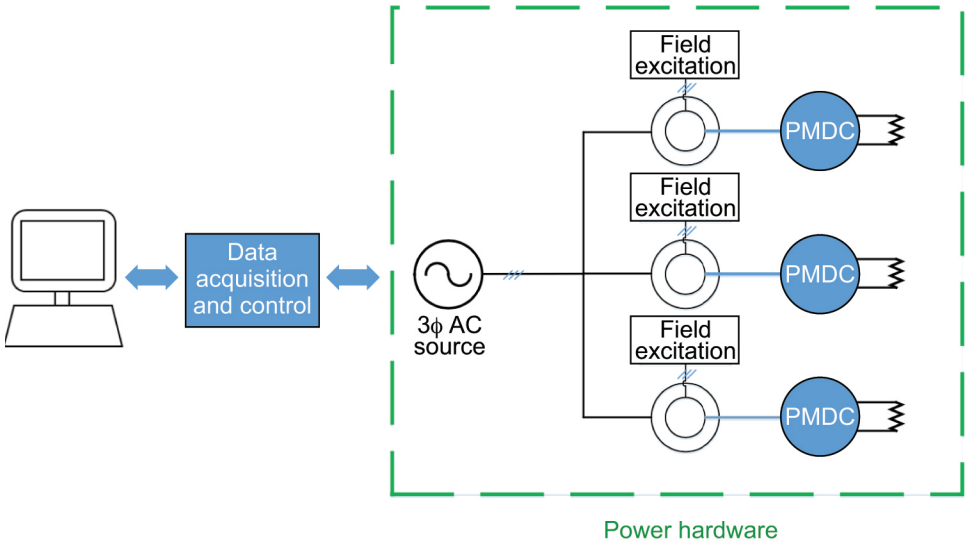

Figure 9.—Low-power testbed structure. Alternating current (AC). Permanent magnet direct current (PMDC). Three phase (3ϕ).

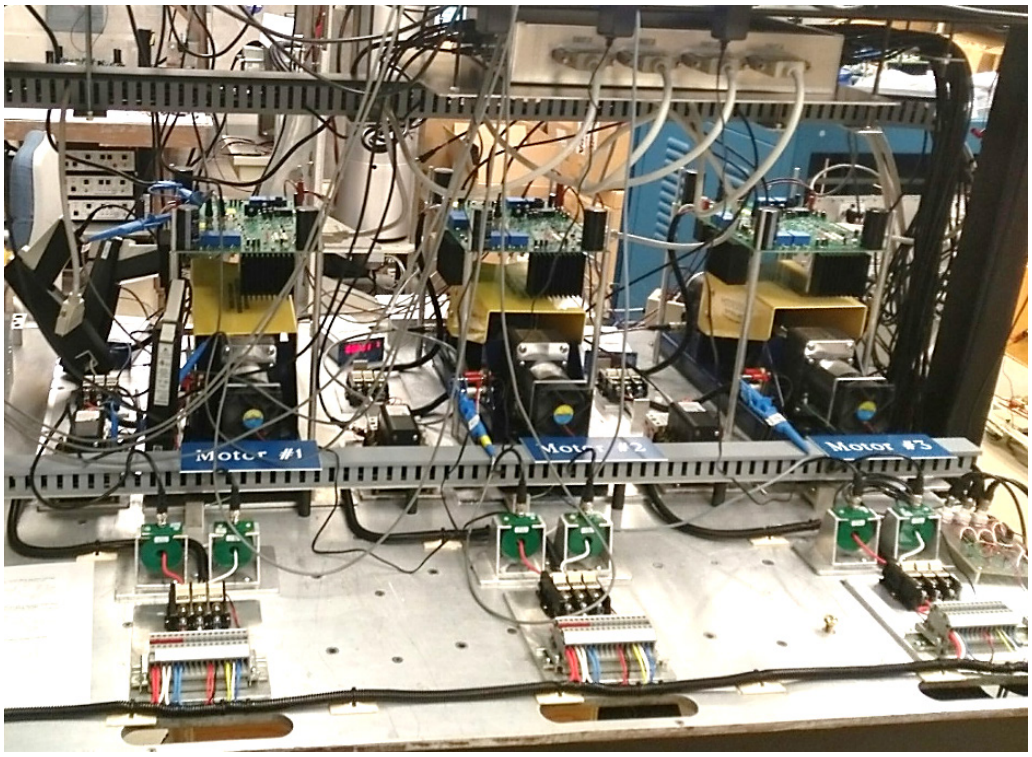

Figure 10.—Low-power testbed power hardware.

5.1 Synchronization

The ability of the DFI motors to synchronize to the grid is demonstrated in Figure 11 and Figure 12, with the motor 2 synchronization as an example. As described previously, the rotor of each machine is excited in such a way that the stator voltages match the bus voltage in magnitude, fundamental frequency, and phase. Once these parameters match, the main contactors are closed, locking the stators of the machines to the grid and enabling closed-loop speed control. In the testbed demonstration, this process was performed manually using filtered signals. For this reason, when the contactor for motor 2 was closed at approximately 3.445 s, a slight transient was encountered, as shown in Figure 11 and Figure 12. The transient is eliminated within 1 s, as one can see the shaft of motor 2 returning to standstill. It is expected that an automated synchronization algorithm would reduce the current and velocity transients further.

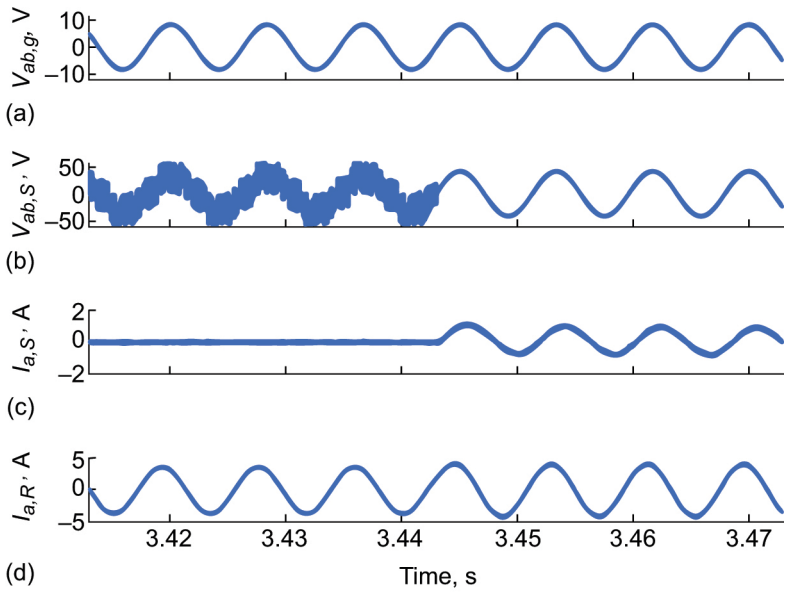

Figure 11.—Doubly fed-induced motor synchronization. (a) Grid voltage ($V_{ab,g}$). (b) Motor 2 stator voltage ($V_{ab,S}$). (c) Stator current ($I_{a,S}$). (d) Rotor current ($I_{a,R}$).

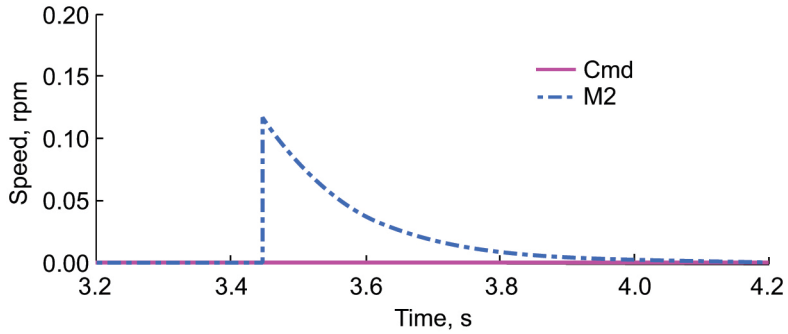

Figure 12.—Motor 2 (M2) speed during synchronization. Command (Cmd).

5.2 Startup

The startup speed curves of the three motors from standstill to synchronous speed at 3,600 rpm are shown in Figure 13, along with the averaged power factor over that time period. Each of the three motors demonstrated balanced operation during the startup transients, and tracked the reference command well. The power factor signal was computed based on filtered signals, and averaged over a number of cycles. The average power factor (not instantaneous) was shown to achieve close to unity power factor operation. The root mean square (RMS) line-to-line voltage and stator and rotor currents are shown in Figure 14 for additional information.

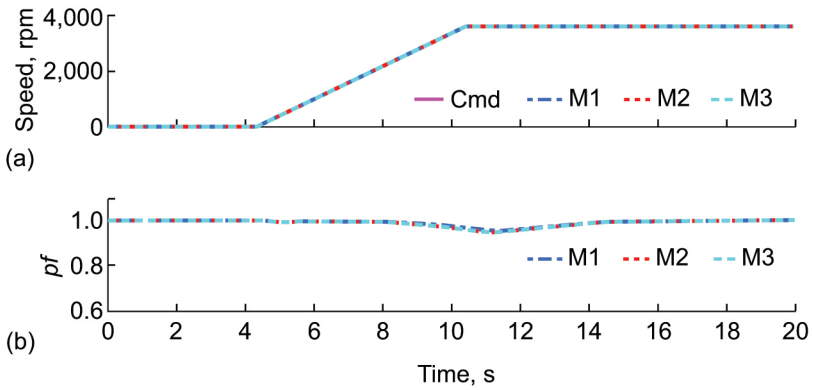

Figure 13.—Three motors (M1, M2, and M3) during startup. (a) Speed reference tracking. Command (Cmd). (b) Averaged unity power factor (*pf*) control.

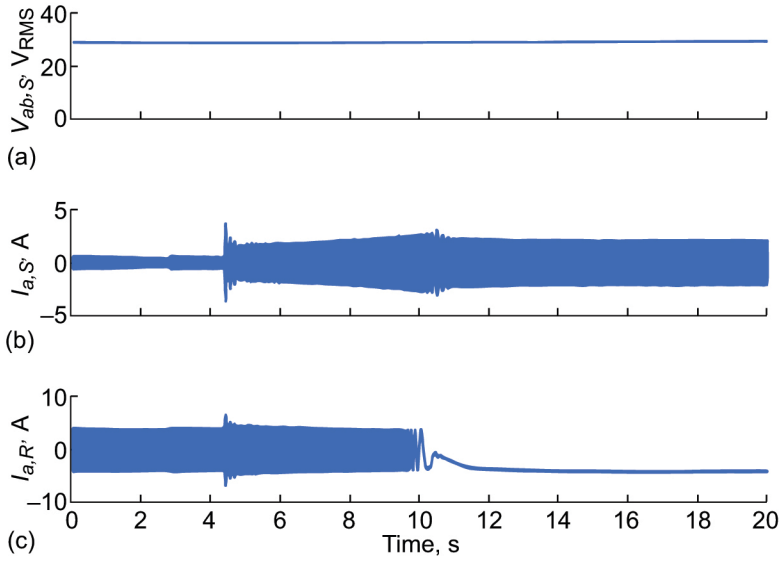

Figure 14.—Voltage and current for stator and rotor. (a) Motor 2 line-to-line root mean square (RMS) stator voltage ($V_{ab,S}$). (b) Phase A stator current ($I_{a,S}$). (c) Phase A rotor current ($I_{a,R}$).

5.3 Differential Operation

The ability for the propulsors to operate simultaneously at different speeds (differential operation), along with transitioning back and forth between differential and concurrent operation is assumed to be necessary for distributed propulsion-based aircraft. This ability, in addition to the averaged power factors of the machines over the noted time, was demonstrated as shown in Figure 15. As one can see, independent from what is occurring with the other machines, the motors track their individual setpoints. In addition, the stator line-to-line RMS voltage, and the stator and rotor currents of motor 2 are highlighted in Figure 16.

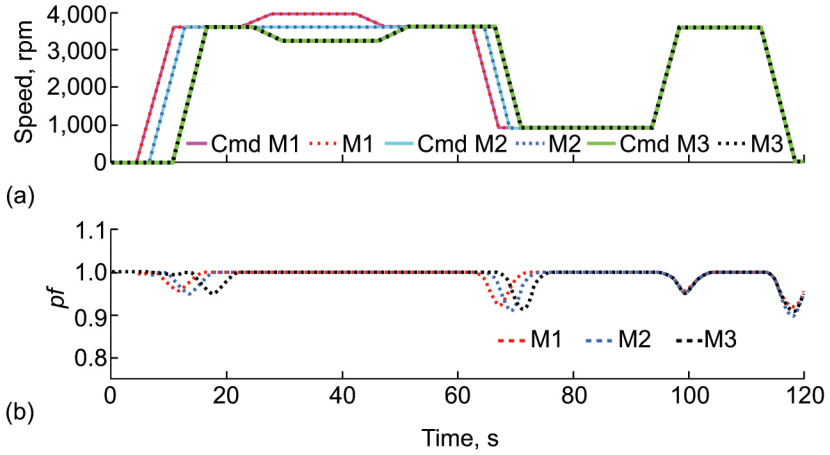

Figure 15.—Speed command setpoint tracking for all three motors (M1, M2, and M3). (a) Differential speed operation. Command (Cmd). (b) Average stator power factor (*pf*).

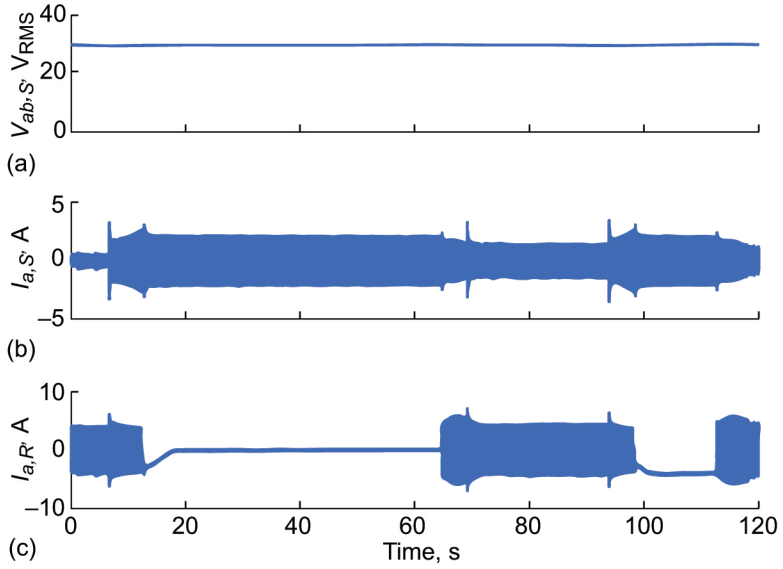

Figure 16.—Motor 2 differential speed tracking. (a) Voltage ($V_{ab,S}$). Root mean square (RMS). (b) Stator current ($I_{a,S}$). (c) Rotor current ($I_{a,R}$).

5.4 Flight Profile Setpoint Tracking

The ability of the propulsors to follow a theoretical flight profile, with the characteristics shown in Figure 17, is shown in Figure 18. The motors track the speed profile with no deviation from the setpoint, and near-average unity power factor at the stator is demonstrated over the duration of the flight profile. The motor 2 voltage and current data is plotted in Figure 19 as done previously.

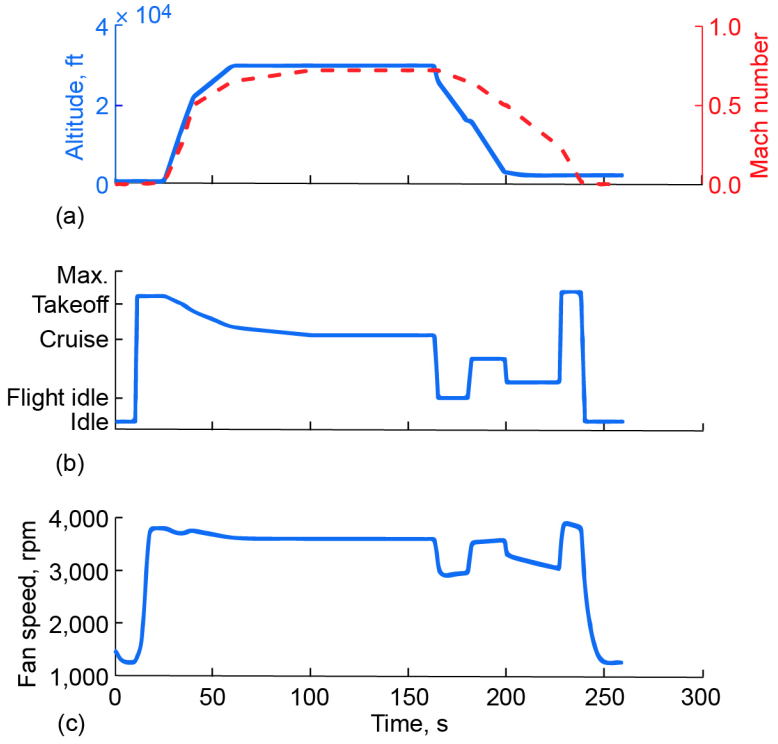

Figure 17.—Parallel motor flight profile. (a) Altitude and Mach number. (b) Throttle. (c) Fan speed.

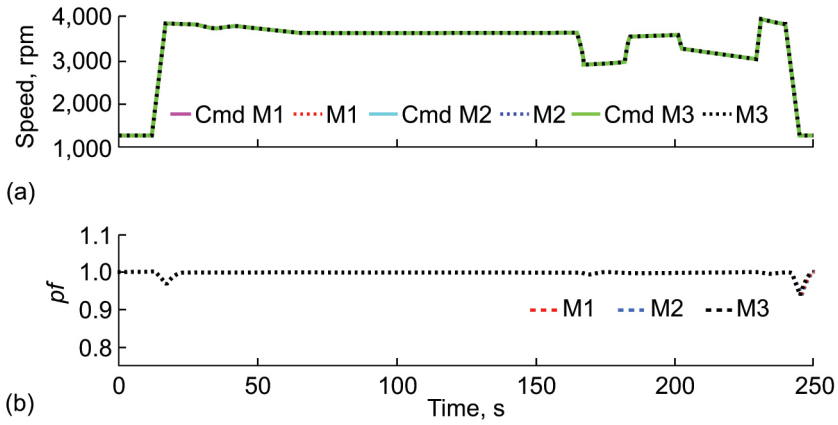

Figure 18.—Flight profile tracking capability, with a 30 line-to-line voltage (VLL), 120 Hz bus. Three motors (M1, M2, and M3). (a) Speed. Command (Cmd). (b) Average unity power factor (*pf*).

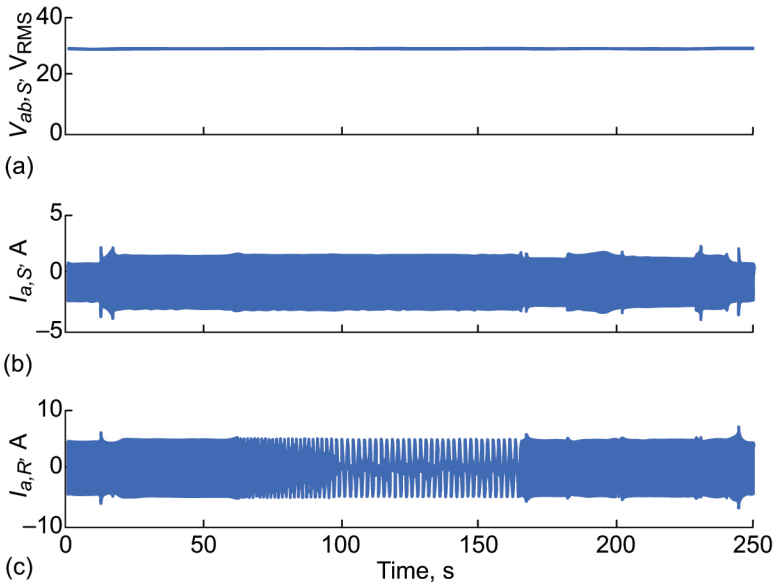

Figure 19.—Motor 2 flight profile. (a) Voltage ($V_{ab,S}$). Root mean square (RMS). (b) Stator current ($I_{a,S}$). (c) Rotor current ($I_{a,R}$).

6.0 Conclusion

The general operating characteristics and control of the doubly fed induction (DFI) motor and its inverter were described and demonstrated in both simulation and experiments. This operation included the DFI motor's ability to synchronize itself to the grid, self-start (with the properly sized power electronics), operate over a wide speed range both synchronously and differentially with other DFI motors on the same bus, and operate with its average power factor at unity during steady-state operation. These characteristics are highly desirable for flight application, allowing similar performance to that of a series driven synchronous or induction machine.

While a DFI motor-based alternating current (AC) power system has been shown to have several positive qualities, there is still research to be done. In the near future, demonstration of a fully doubly fed induction machine- (DFIM-) based system with the DFIM as the generator and the motor(s) will be reported utilizing the low-power testbed. In addition, more accurate loading models are necessary to represent in-flight fan load dynamics and the respective sizing of the rotor-side converter (RSC) for such a load, since the testbed bandwidth limitations only allowed for a linear torque-speed curve to be implemented. After that, studies need to be performed regarding the performance of the AC system in relation to the stiffness of the AC bus, DFIM scaling to high-power and possibly high-speed operation, brushless concepts, and so on. These efforts will all lead into potential medium (several hundred kilowatts) and/or high-power tests (megawatt) for future aircraft electric propulsion.

References

1. National Aeronautics and Space Administration: NASA Aeronautics: Strategic Implementation Plan 2017 Update. 2017. https://www.nasa.gov/sites/default/files/atoms/files/sip-2017-03-23-17-high.pdf Accessed May 9, 2017.
2. Armstrong, Michael J., et al.: Architecture, Voltage, and Components for a Turboelectric Distributed Propulsion Electric Grid: Final Report. NASA/CR—2015-218440 (EDNS04000038188/002), 2015. http://ntrs.nasa.gov

3. Sadey, David J.; Taylor, Linda M.; and Beach, Raymond F.: Proposal and Development of a High Voltage Variable Frequency Alternating Current Power System for Hybrid Electric Aircraft. AIAA 2016–4928, 2016.
4. Muller, S.; Deicke, M.; and De Doncker, Rik W.: Doubly Fed Induction Generator Systems for Wind Turbines. IEEE Ind. Appl. Mag., vol. 8, no. 3, 2002, pp. 26–33.
5. Dick, Barry: New Technology for Speed Control of Wound Rotor Motors. IEEE Cement Industry Technical Conference, 2006.
6. Yuan, Xibo: Chai, Jianyun; and Li, Yongding: A Converter-Based Starting Method and Speed Control of Doubly Fed Induction Machine With Centrifugal Loads. IEEE Trans. Ind. Appl., vol. 47, no. 3, 2011, pp. 1409–1418.